Batch equilibrium and kinetics of mercury removal from aqueous solutions using polythiophene/graphene oxide nanocomposite

Anthony M. Muliwa, Maurice S. Onyango, Arjun Maity and Aoyi Ochieng

ABSTRACT

Polythiophene/graphene oxide (PTh/GO) nanocomposite (NC) was prepared through polymerisation of thiophene in the presence of GO and was used for mercury ions (Hg^{2+}) adsorption in aqueous solutions. Equilibrium studies showed that mercury removal was strongly influenced by solution pH and GO composition in the NC. The equilibrium data were well described by both Langmuir and Freundlich isotherm models, with a Langmuir maximum adsorption capacity of 113.6 mg/g. Adsorption kinetics were rapid and correlated well with the pseudo-second-order model. The thermodynamic studies indicated that the adsorption was spontaneous and endothermic in nature, and occurred through a physicochemical mechanism. Desorption studies revealed that PTh/GO NC could be used repeatedly for three adsorption-desorption cycles without a significant loss in its capacity. Competing ions reduced mercury uptake although considerable values were still attained. The findings of this study suggest that PTh/GO NC is a potential adsorbent for Hg^{2+} removal from aqueous solutions.

Key words | adsorption, graphene oxide, mercury, nanocomposite, polythiophene

Anthony M. Muliwa (corresponding author)
Maurice S. Onyango
Arjun Maity
Department of Chemical, Metallurgical and Materials Engineering,
Tshwane University of Technology,
Private Bag X680,
Pretoria,
South Africa
E-mail: *muliwaam@tut.ac.za*

Arjun Maity
DST/CSIR National Centre for Nanostructured Materials,
Council for Scientific and Industrial Research,
Pretoria,
South Africa

Aoyi Ochieng
Centre for Renewable Energy and Water,
Vaal University of Technology,
Vanderbijlpark,
South Africa

INTRODUCTION

Water pollution through mercury emissions is of great environmental concern due to its high toxicity and detrimental effect on human and aquatic life. Pollution of water by mercury occurs mainly through discharge of effluent streams from industries such as paint making, electrical, pulp and paper, fertiliser, rubber processing, chloro-alkali, coal-fired power plants and ore mining (Moghaddam & Pakizeh 2015). In aqueous solution, mercury exists mainly in the form of elemental mercury (Hg) and ionic mercury (Hg^{+} and Hg^{2+}) species (Lottermoser 2010). Mercury is considered as one of the most toxic heavy metals on earth, and is listed as a priority pollutant by the US Environmental Protection Agency (USEPA 2014). Mercury has the ability to bind to the amino acid cysteine proteins, resulting in serious neurological damage to both human and aquatic life. Due to its high toxicity, the World Health Organization (WHO) has set the tolerance limit for mercury in drinking and surface water at 1 μg/L and 10 μg/L, respectively (WHO 1990). Thus, environments having a mercury concentration above the recommended limits require application of a proper treatment regime.

The conventional treatment methods used in the removal of mercury from effluent streams include sulphide precipitation (USEPA 2007), the Blue PRO® reactive filtration process (Shafeeq *et al.* 2012), membrane processes (Sharma *et al.* 2015), coagulation (Henneberry *et al.* 2011), biofilms (Bhattacharya *et al.* 2016) and the adsorption process (Yu *et al.* 2016). Among these treatment technologies, adsorption has been reported as the most robust due to its simplicity, ease of operation and environmental benignity (Cui *et al.* 2015). A number of adsorbents such as activated carbon (Ekinci *et al.* 2002; Yardim *et al.* 2003), bicarbonate treated peanut hull carbon (Namasivayam & Periasamy 1993), thiol-functionalised mesoporous silica microspheres (Bibby & Mercier 2002), iron hydrous oxide gel (Kinniburgh & Jackson 1978), and thiol derivatised single wall carbon nanotubes (Bandaru *et al.* 2013), have been employed in the removal of Hg^{2+} from aqueous solutions. However, the aforementioned materials suffer from limitation such as inherently low capacity, slow removal kinetics and poor selectivity. Consequently, there is an urgent need to design and develop novel materials

doi: 10.2166/wst.2017.165

with desirable attributes such as enhanced capacity, fast removal kinetics, and high reusability.

Recently, a lot of effort has been geared towards use of nanocomposite (NC) materials for environmental remediation due to the synergistic effects of the individual components and the improved affinities towards metal ions. The development of NC focuses mainly on tailoring the physicochemical properties of materials to enhance contaminant selectivity. Conducting polymers have been used to decorate functional groups such as amine, thiol and carboxyl onto nanoadsorbent surfaces. These functional groups are beneficial in the decontamination of effluent streams. Among the conducting polymer family of polypyrrole (PPy), polyaniline (PANI) and polythiophene (PTh), few studies have reported the use of PTh for heavy metals removal from aqueous environments. PTh, and their composites, have been extensively used for optical, electronic and mechanical applications (Uygun *et al.* 2009; Wayne *et al.* 2010; Bobade 2011; Kumar *et al.* 2015). Thus it is important to investigate the possibility of using PTh-based materials in the removal of contaminants. The structure of PTh contains abundant sulphur atoms bonded to two carbon atoms on either side, leaving two un-bonded lone pairs of electrons exposed. Thus it is capable of donating a pair of electrons to a Lewis acid such as Hg^{2+}, hence forming a chelate. In this case, mercury acts as an electron acceptor while the sulphur atom acts as an electron donor, according to the principle of hard soft acids and bases (HSAB) (Pearson 1963; Nabais *et al.* 2006; Wajima & Sugawara 2011). However, PTh has poor dispersion characteristics and a low surface area, resulting from particle agglomerations. Hence, a support material is required to improve its properties.

Carbon-based nanomaterials, for instance GO, are currently receiving a great deal of attention as adsorbents and also as polymer host materials for abatement of inorganic and organic pollutants from aqueous solutions. Graphene oxide (GO) offers utility in various applications because of its unique 2D features and bond structure (Sheet *et al.* 2014). Remarkable properties such as the presence of surface functional groups (carboxyl, hydroxyl, epoxide and carbonyl) and large specific surface area make GO and their composites highly potential adsorbents for water purifications (Nuengmatcha *et al.* 2014). Therefore, a NC prepared by combining GO and PTh could result in an adsorbent material with dramatic improvements in physicochemical properties such as high surface area, improved dispersion characteristics and enhanced mercury ion pollution clean-up. Although a few sulfurised adsorbents for Hg^{2+} removal from aqueous solutions have previously been reported (Nabais *et al.* 2006; Wajima & Sugawara 2011), their preparation procedures were tedious and time-consuming. Moreover, toxic H_2S gas and very high temperatures were utilised, necessitating careful control. Similarly, the reported GO was mainly prepared through hazardous methods that are susceptible to explosions and release of toxic gases such as NO_2, N_2O_4, and/or ClO_2 (Marcano *et al.* 2010). Therefore, there is an urgent need to develop green methods for preparation of high yield dispersible PTh/GO NC with improved properties suitable for Hg^{2+} adsorption.

Consequently, this study seeks to synthesise, characterise and evaluate the performance of PTh/GO NC in the removal of mercury ions from aqueous solutions. GO sheets were synthesised from graphite flakes using a modified method reported by Marcano *et al.* (2010), and thereafter, the as-prepared GO was functionalised by PTh via an *in situ* interactive polymerisation method. The influence of pH, adsorbent dosage, initial concentration and temperature on Hg^{2+} adsorption were explored by performing batch equilibrium isotherms and kinetics experiments. Lastly, desorption and competitive adsorption were studied and a plausible Hg^{2+} removal mechanism was proposed.

MATERIALS AND METHODS

Materials

Graphite flakes (325 mesh, 99.95% purity), anhydrous iron (III) chloride ($FeCl_3$), potassium permanganate ($KMnO_4$), chloroform ($CHCl_3$), thiophene (Th) monomer (C_4H_4S, density = 1.051 g/cm^3, ≥99%), hydrogen peroxide (H_2O_2, 30 wt.% ACS reagent) and mercury dichloride ($HgCl_2$) salt were all purchased from Sigma-Aldrich (Germany). A stock solution (1 L) of 1,000 mg/L of Hg^{2+} was prepared by dissolving 1.354 g of $HgCl_2$ in deionised water (Purite water system, Model Select Analyst HP40, UK) acidified with 5 mL concentrated HNO_3 to prevent hydrolysis. All pH adjustments were done with either 0.1 M HNO_3 or 0.1 M NaOH solution. Other chemicals were of analytical reagent (AR) grade.

Preparation of GO nanosheets

GO nanosheets were prepared using an improved method described elsewhere (Marcano *et al.* 2010). In brief, the following stoichiometric ratios were used in the synthesis of GO sheets; H_2SO_4: graphite flakes (100:1, v/w); $KMnO_4$:

H_2SO_4 (1:20, w/v); H_3PO_4: H_2SO_4 (1:9, v/v). First, 3.6 g was added to 400 mL of H_3PO_4/H_2SO_4 mixture in a 1,000 mL glass beaker. $KMnO_4$ (18 g) was then added gradually into the graphite-acid mixture to prevent overheating. The mixture was kept under stirring and the temperature rose to about 35–40° C. The mixture was heated further to 50 °C and maintained at that under constant stirring for 12 h. The brown mixture was then poured into 460 mL of ice and 5 mL of 30 wt.% H_2O_2, resulting in a bright-yellow colour and temperature increase to about 98°C. Finally, GO nanosheets were obtained through ultrasonic agitation after the mixture had been filtered and thoroughly washed using HCl and deionised water, until pH of the filtrate was 7.

Preparation of the PTh/GO NC

PTh/GO NC was prepared by first dispersing 0.4 g of GO nanosheets in 30 mL of chloroform in a conical flask under sonication for 30 minutes. Thereafter, 0.95 mL of thiophene monomer was injected into the reaction mixture while stirring magnetically for further 30 minutes. To this mixture, $FeCl_3$ (8 g) was poured in one go and left for 6 h under stirring at room temperature. Thereafter, the obtained suspension was vacuum filtered and repeatedly rinsed with deionised water and methanol, until the pH of the colourless filtrate was 7. Finally, the solid materials (PTh/GO NC) were vacuum dried at 60 °C for 24 h. The total mass of NC was 1.4 g, and the compositions of GO and PTh were 28.5 wt.% and 71.5 wt.%, respectively. Similarly, PTh/GO NC was prepared using different masses (0.1, 0.2, 0.6, 0.8 g) of GO and were designated as 9.1, 16.7, 37.6 and 44.4 wt.%, respectively, based on GO composition in the NC.

Characterisation of the PTh/GO NC

Brunauer–Emmett–Teller (BET) measurements were recorded on PTh and PTh/GO NC with a Micromeritics TRISTAR 3,000 surface area analyser using the N_2 adsorption-desorption method (−196°C). The morphological characteristics and elemental compositions were analysed using a field emission scanning electron microscope (FE-SEM, JEOL JSM-7600F) equipped with energy dispersive X-ray (EDX). Information on functional groups was obtained by Fourier transform infra-red (FT-IR) spectrometer, while zeta potentials were measured using a ZETASIZER nano-series (Nano ZS-90, Malvern Instruments, UK) at different pHs.

Adsorption studies

Batch equilibrium experiments were performed in a temperature-controlled thermostatic bath shaker operated at 160 rpm. In brief, the effect of solution pH (2–10), adsorbent mass (10–120 mg), initial concentration (50–500 mg/L), temperature (25–45 °C) and co-existing ions (Cu, Mn, Zn) on the adsorption of Hg^{2+} onto PTh/GO NC was investigated. The effect of pH on Hg^{2+} removal was explored by contacting 50 mL of 100 mg/L Hg^{2+} solution with 80 mg of either PTh or PTh/GO NC contained in 100 mL plastic bottles. The samples were shaken continuously for 24 h at 25 °C, and thereafter the suspension was filtered with 0.45 μm cellulose acetate syringe filters. The residual concentration of Hg^{2+} ions in the filtrate was analysed using an inductively coupled plasma atomic emission spectrometer (ICPE-9000, Shimadzu). A similar procedure was adopted to investigate the effect of the remaining variables. The mercury removal efficiency, R_o(%) and the uptake, Q_e (mg/g) at equilibrium were determined using Equations (1) and (2), respectively:

$$R_o(\%) = \frac{(C_o - C_e)}{C_o} \times 100 \quad (1)$$

$$Q_e = \frac{(C_o - C_e)}{m} V \quad (2)$$

where C_o and C_e are the initial and equilibrium concentrations of Hg^{2+} (mg/L) in the liquid phase, respectively, while m and V are the adsorbent mass (g) and the volume (L) of the solution used. The effect of coexisting ions such as zinc (Zn), copper (Cu) and manganese (Mn) on mercury adsorption was also investigated in binary, ternary and multicomponent systems by varying their initial concentration.

Adsorption kinetics experiments were conducted by placing 1.6 g of PTh/GO NC in 1 L vessels containing Hg^{2+} solutions of different concentrations (50, 100, 200 mg/L). The suspensions were kept under stirring at constant speed (160 rpm) and temperature (25 °C). At predetermined time intervals, 1 mL samples were collected, filtered and analysed for Hg^{2+} ion concentration. The Hg^{2+} uptake, Q_{ti} (mg/g) at any time t_i was computed as follows:

$$Q_{t_i} = \frac{(C_o - C_{t_i})V_o - \sum_2^{i-1} C_{t_{i-1}} V_s}{m} \quad (3)$$

where C_{t_i} (mg/L) is the liquid-phase concentrations of Hg^{2+} at any time t_i (min), V_o is the total solution volume (L) before sampling and V_s is the volume (0.001 L) of the withdrawn samples at time t_i.

Desorption studies

Desorption and regeneration tests were conducted by first adding 0.08 g of the PTh/GO NC in different 50 mL solutions of Hg^{2+}, contained in 100 mL plastic sample bottles. Each solution had an Hg^{2+} concentration of 100 mg/L and pH 6. These samples were shaken for 24 h at constant temperature (25 °C) to attain equilibrium. Thereafter, the samples' contents were mixed together and the mercury-bound PTh/GO NC was separated by centrifugation, rinsed with distilled water to remove any unadsorbed Hg^{2+} ions, and dried in a vacuo at 60 °C. This mercury-bound PTh/GO NC was dispersed in 0.5 M solutions of either HCl, H_2SO_4 or HNO_3 (serving as eluting agents) and placed in the thermostatic shaker for 24 h. After that, the adsorbent was separated and the supernatant was measured for Hg^{2+} ions. Then desorption efficiency was calculated by performing appropriate mass balances. In another set of experiments, the used-adsorbent was first activated by suspending it in 1 M NaOH solution for 3 h, before conducting four subsequent adsorption-desorption experiments.

RESULTS AND DISCUSSION

Adsorbent characterisation

Specific surface area is one of the key parameters that determine the performance of any adsorbent. The BET surface area, total pore volume and pore size of PTh and PTh/GO NC are listed in Table S1 (supplementary file, available with the online version of this paper). The specific surface area of PTh/GO NC (42.81 m^2/g) was found to be higher than that of PTh (18.23 m^2/g). The increased surface area can be attributed to the synergistic effect of GO in the NC, and it correlated well with the enhanced Hg^{2+} adsorption performance onto PTh/GO NC. Also, the total pore volume and the average pore size decreased from 0.2487 to 0.0950 m^3/g and from 43 to 36 nm, respectively. These results are consistent with previous works (Setshedi *et al.* 2015).

The FT-IR spectrum of GO shown in Figure 1(c) displays a broad peak at 3,300 cm^{-1}, which is due to O-H stretching vibrations, C = C arising from un-oxidised sp^2 bonds at 1,625 cm^{-1}, and C-O vibrations at 1,235 cm^{-1} (Shen *et al.* 2009; Marcano *et al.* 2010), confirming the existence of carboxyl, epoxy and alkoxy groups in GO, respectively. The FT-IR spectrum of PTh/GO NC before adsorption (Figure 1(a)), shows peaks of C-S-C and C-S bending and

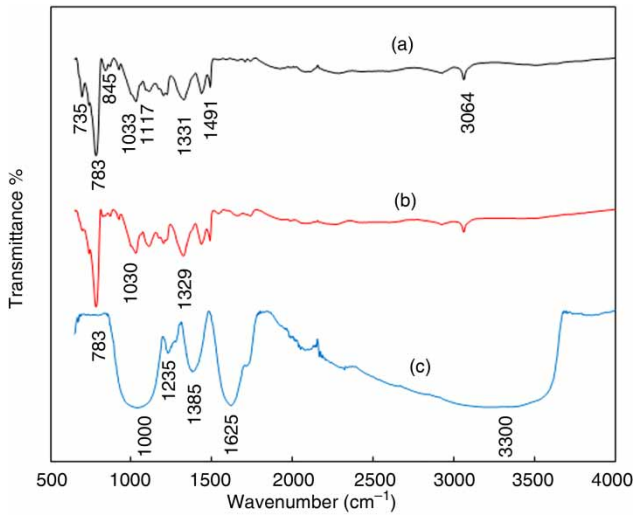

Figure 1 | FT-IR spectra of GO (a) and PTh/GO NC before (b) and after (c) mercury adsorption.

stretching vibration (735–845 cm^{-1}), C-H out-of-plane bending vibrations (783 cm^{-1}), C = C symmetric vibrations (1,491 cm^{-1}) and C-H in-plane bending vibrations of thiophene (1,033–1,117 cm^{-1}). The peak at 3,064 cm^{-1} is attributed to interactions between the OH in the GO and PTh. Moreover, a comparison of the spectra of GO and PTh/GO NC revealed a dramatic decrease in intensity of the absorption peaks of oxygen-containing functional groups; a probable indication that GO was partially reduced (Lee *et al.* 2010; Mehdinia *et al.* 2015). These findings confirmed that PTh/GO NC was successfully synthesised. After Hg^{2+} adsorption onto the PTh/GO NC (Figure 1(b)), the characteristic peak at 735 cm^{-1} ascribed to C-S-C stretching slightly shifted to 721 and decreased in intensity, suggesting that S may have interacted with Hg^{2+} ions.

Figure 2 shows the FE-SEM micrographs of GO, PTh and PTh/GO NC. Figure 2(a) is an image of GO, showing thin-wrinkled sheets of varying size and shape. Figure 2(b) is for PTh, and it illustrates nearly spherical agglomerated particles. As for PTh/GO NC (Figure 2(c)), the surface is rough, with granular depositions, and GO sheets are no longer visible, thus confirming the presence of PTh in the NC. The EDX spectra of PTh/GO NC, before and after Hg^{2+} ion adsorption, were recorded as shown in Figures S1(a) and S1(b) (supplementary file, available with the online version of this paper). The presence of mercury characteristic peaks at 2.195 and 9.987 keV confirms the affinity of PTh/GO NC towards mercury. These results are in good agreement with the findings of Saleh (2015). However, peaks of P, Cl, Fe are present in the NC as a result of using $FeCl_3$ oxidant and H_3PO_4 in the synthesis of GO.

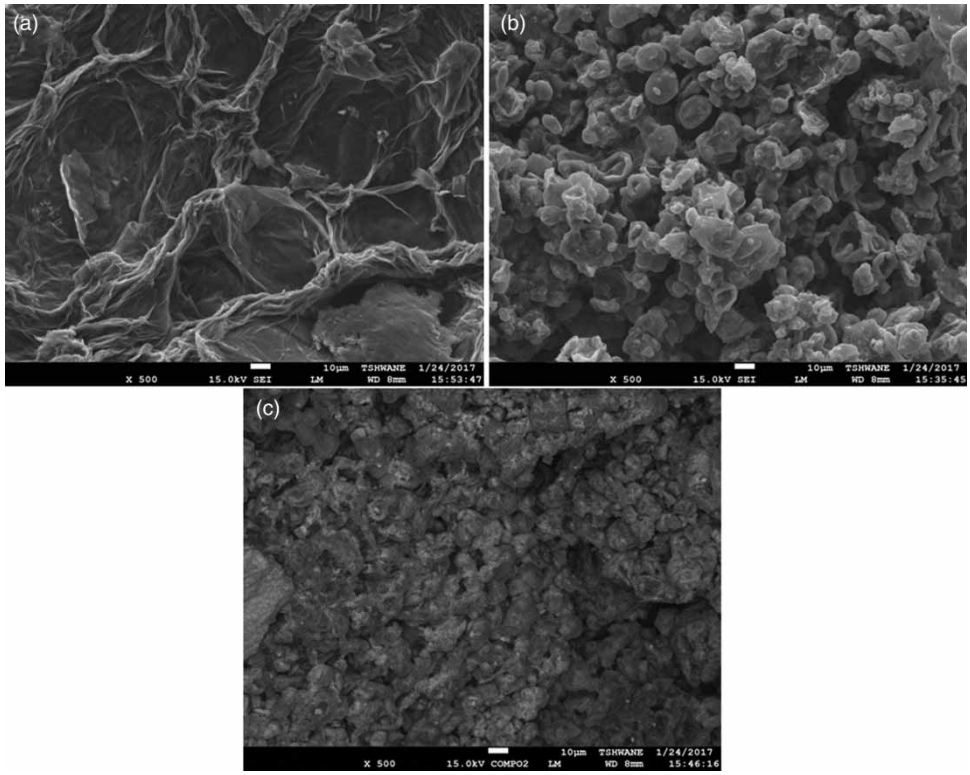

Figure 2 | Scanning electron micrographs of (a) GO, (b) PTh and (c) PTh/GO NC.

The presence of these impurities indicates that the NC is not pure and contains doped ions. Table S2 (supplementary file) lists the elemental compositions of GO, PTh and PTh/GO NC.

To verify the surface charges on the as-prepared adsorbents, zeta potentials were measured at different pHs. As shown in Figure S2 (supplementary file), zeta potentials of PTh/GO NC were less negative than those of GO over the whole measured pH range. For both materials, the zeta potential declines from positive values at acidic pHs to negative values. This decline can be attributed to protonation and deprotonation effects. The isoelectric point of PTh/GO NC was found at pH 5, and the composite exhibited significantly enhanced the carrying capacity of hydrogen ions because of the ability of sulphur atoms to adsorb hydrogen ions. Consequently, many hydroxyl ions were required to neutralise hydrogen ions on PTh/GO NC, resulting in a remarkable increase in isoelectric point. On the other hand, GO did not exhibit any isoelectric point within the studied pH range (Yan *et al.* 2014). Therefore, at pH > 5, PTh/GO NC was negatively charged and at pH < 5, it was positively charged. These observations are consistent with the increased Hg^{2+} ion removal as pH increases.

Batch equilibrium and adsorption kinetic studies

Effect of the GO loading on mercury removal

To determine the optimum ratio of GO to PTh constituents for Hg^{2+} ion adsorption, PTh/GO NC with different GO loadings (9.1–44.4 wt.%) were synthesised and used in preliminary batch tests. The optimised results (Figure 3) show that 28.5 wt.% GO material achieved the highest removal efficiency of Hg^{2+} (100%), while the control (pure GO) achieved only 42% mercury removal. Therefore, the adsorbent with the 28.5 wt.% GO loading was selected and used in all subsequent adsorption studies.

Effect of pH and adsorbent dose on mercury removal

The adsorption of metal ions is strongly influenced by the pH of the solution. pH affects ionisation of the functional groups on an adsorbent surface as well as the speciation of ions in the solution thus affecting the entire adsorption process (Carrott *et al.* 1998). Figure 4 shows a combined plot of the effect of pH and adsorbent dose on the removal of Hg^{2+} ions from aqueous solution using PTh/GO NC. The results indicate that the removal of Hg^{2+} ions from the aqueous

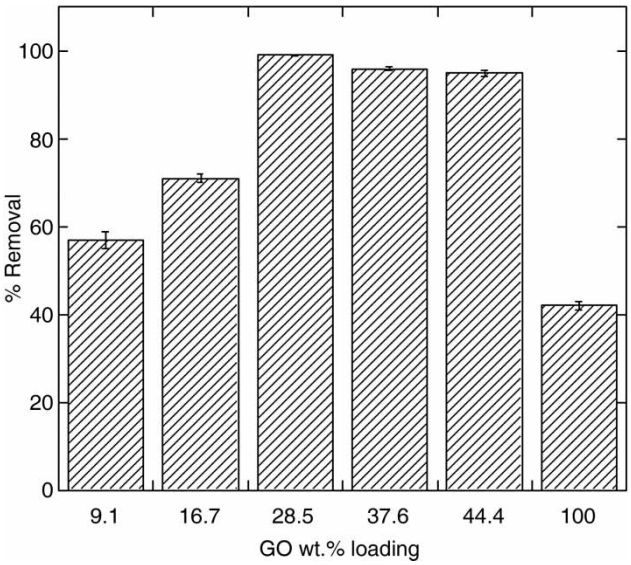

Figure 3 | Effect of GO percentage loading on Hg^{2+} ions removal ($C_o = 100$ mg/L, Temp = 25 °C, pH = 6).

solution by PTh/GO increased with an increase in pH, achieving total removal at neutral pH. Beyond pH 7, there was a decrease in Hg^{2+} ions removal. The observed removal trend could be due to the fact that in the presence of Cl^- ions and at pH < 4, the predominant mercury species is $HgCl_2$ while at pH > 4, it exists in $Hg(OH)_2$ form (Knocke & Hemphil 1981). The decline in Hg^{2+} removal at pH > 7 may be due to the formation of water soluble complexes such as $Hg(OH)_3^-$ and $Hg(OH)_4^-$ which are difficult to remove (Yardim *et al.* 2003; Moghaddam & Pakizeh 2015). Therefore, all subsequent experiments were conducted at pH 6 and 80 mg of adsorbent dose.

Effect of initial concentration and temperature

Figure 5 shows a combined plot of the effect of initial Hg^{2+} concentration (when the initial concentrations (50–500 mg/L) and temperature (25–45 °C) on the uptake of Hg^{2+} ions by PTh/GO NC. It can be seen that the uptake increases with increase in initial concentration. The increase in Hg^{2+} uptake is attributed to the fact that the concentration gradient is the driving force in the adsorption, thus increasing concentration increases the concentration gradient. Moreover, increase in concentration resulted in increased interactions between Hg^{2+} ions and active sites of PTh/GO NC.

Mercury uptake increased with increase in temperature. This can be attributed to the fact that an increase in kinetic energy of mercury ions in aqueous solution enhances the solid-liquid interaction. Moreover, at high temperatures, there is less resistance offered to the fast moving Hg^{2+} ions by viscous forces in the aqueous phase.

Adsorption isotherm modelling

Adsorption isotherms provide useful information regarding the capacity of an adsorbent as well as the description of the functional dependence of capacity on the concentration

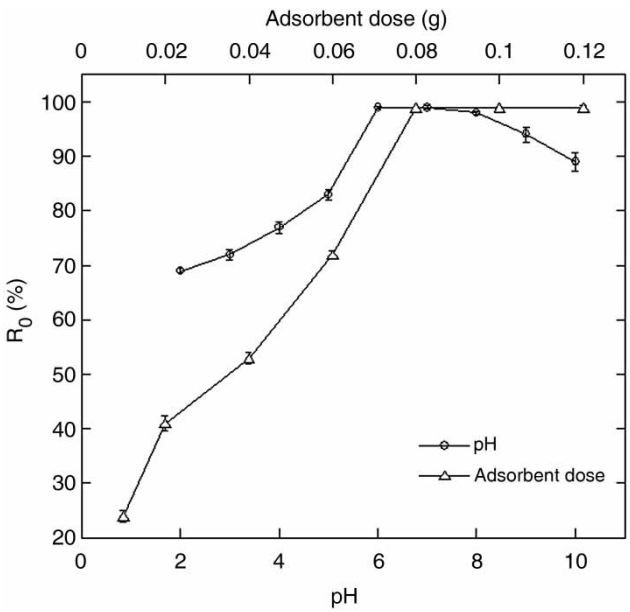

Figure 4 | The effect of pH and adsorbent mass on the removal of Hg^{2+} ions by PTh/GO NC ($C_o = 100$ mg/L, Temp = 25 °C, Vol = 50 mL).

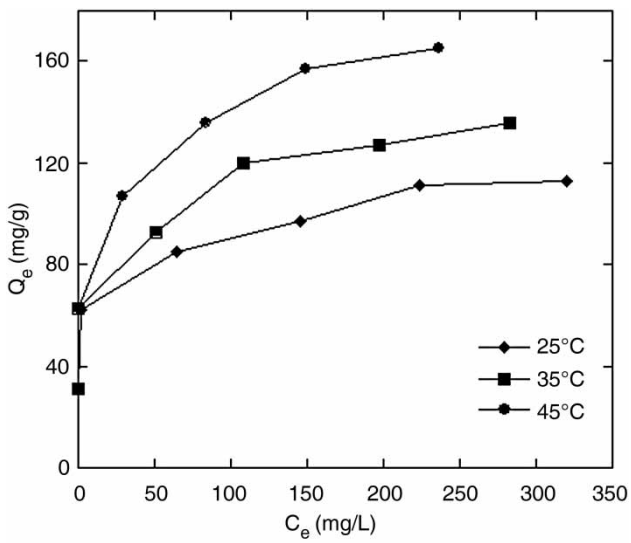

Figure 5 | Effect of initial concentration and temperature on mercury uptake by PTh/GO NC (adsorbent dose = 0.08 g/50 mL, pH = 6).

of the pollutant. The equilibrium data were analysed using Langmuir, Freundlich, Tempkin and Dubinin–Radushkevich (D-R) (Foo & Hameed 2010), listed as Equations (S1)–(S4), respectively (supplementary file, available with the online version of this paper). Non-linear fits of Langmuir and Freundlich models (inset is linear Langmuir model) are shown in Figure S3(a), while the linear forms of D-R, Freundlich and Tempkin models are plotted in Figure S3(b), Figures S4(a) and S4(b) (supplementary file), respectively. Parameters extracted from linearised and non-linearised isotherm models are presented in Table 1 and Table S3 (supplementary file), respectively. Based on the linear regression analysis, R^2 values obtained from the Langmuir isotherm model were higher ($R^2 > 0.99$) than those from Freundlich and Tempkin models, suggesting that the experimental data are best described by the Langmuir model. Further, values of separation factor (R_L) (not shown) were within $0 < R_L < 1$, range, confirming that adsorption is favourable. The Langmuir adsorption capacity for the PTh/GO NC was 113.64 mg/g which is comparably high to other adsorbents reported in the literature (Table S4 in the supplementary file). On the other hand, non-linear regression analysis gave low values of R^2 for both the Langmuir and Freundlich models, although the Freundlich model gave slightly higher values of R^2. This discrepancy of R^2 values obtained might be due to the inherent limitations of linear regression method. Realistically, the Freundlich isotherm, which is based on the assumption of a heterogeneous surface, described the adsorption of mercury onto PTh/GO NC satisfactorily and the adsorption was also favourable ($0 < 1/n < 1$). In addition, the mean free energy values obtained from the D-R model (7.89, 8.39 and 12.61 kJ/mol) suggested that the adsorption of mercury onto PTh/GO NC may have occurred through a physicochemical mechanism (Raji & Pakizeh 2013).

Thermodynamic parameters given in Table 1 were obtained from Van 't Hoff's plot (Figure S5) and Equations S5 and S6 (supplementary file). The values of Gibb's free energy (ΔG) decreased from −0.166 to −2.5407 kJ/mol, when the temperature was increased from 25 to 45 °C, implying that the adsorption process was feasible and spontaneous in nature. The positive values of enthalpy (ΔH) and entropy (ΔS) changes stated that the adsorption process was endothermic, and the randomness at the solid-liquid interface increased during adsorption, respectively.

Adsorption kinetic studies

The study of adsorption kinetics is an important undertaking towards sorption system design because the system's

Table 1 | Linearised isotherms' and thermodynamic parameters

Temp °C	Langmuir			Freundlich			Tempkin			D-R			Thermodynamics		
	Q_{max}	k_L	R^2	$1/n$	K_F	R^2	RT/b_T	A_T	R^2	E	β	Q_e	R^2	ΔG	ΔH	ΔS
25	113.64	0.109	0.993	0.185	39.22	0.965	18.22	1.617	0.960	7.89	8.03E − 09	124.18	0.956	−0.166	35.25	118
35	135.68	0.117	0.992	0.212	41.87	0.933	23.86	1.103	0.951	8.39	7.11E − 09	153.85	0.973	−1.473		
45	166.67	0.131	0.992	0.214	52.42	0.989	28.57	1.453	0.992	12.61	6.29E − 09	185.69	0.992	−2.541		

Note: All isotherms' parameters and their respective units are defined in the supplement (available with the online version of this paper).

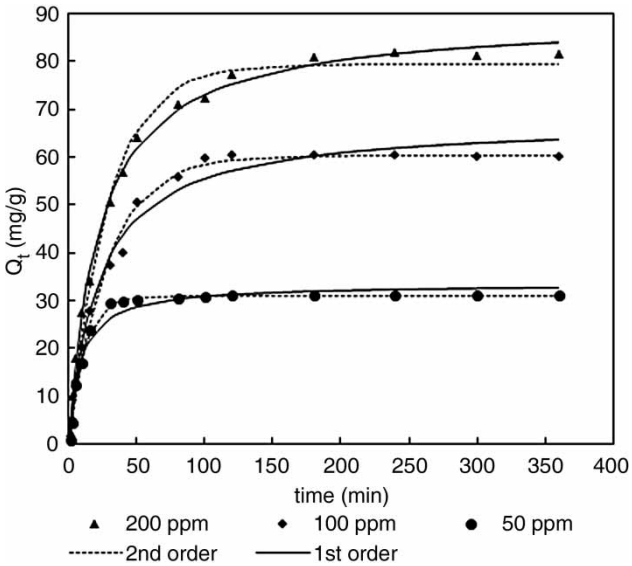

Figure 6 | Effect of initial Hg^{2+} ions concentration on adsorption kinetics and non-linear fitting of pseudo-first-order and pseudo-second-order kinetic models (adsorbent dose = 1.8 g/L, Temp = 25 °C, speed = 160 rpm, Vol = 1,000 mL).

kinetics control the adsorbate residence time and the reactor dimensions (Chowdhury & Saha 2011). In this study, the effect of initial Hg^{2+} ion concentration and contact time on adsorption capacity was investigated and the results are shown in Figure 6. Rapid uptake of mercury is evident in the initial stages, followed by a gradual uptake as the system approaches equilibrium at the prevailing conditions. The rapid uptake can be attributed to the availability of more active sites and the existence of a greater concentration gradient.

The adsorption kinetic data were fitted to the following kinetic models; pseudo-first-order and pseudo-second-order models (Qiu *et al.* 2009) listed as Equations (S7) and (S8) in the supplementary file (available online). Figure 6 shows non-linear kinetics plots while Figure S6 (supplementary file) shows the linear kinetic plots for the removal of Hg^{2+} from aqueous solution. The kinetic parameters obtained from both non-linear and linear models are summarised in Table 2 and Table S5 (supplementary file), respectively. Comparatively, the pseudo-second-order model had the highest coefficient value ($R^2 > 0.99$) among the tested kinetic models, suggesting that the adsorption proceeds via the pseudo-second-order kinetics. Moreover, the theoretical equilibrium capacities (Q_{ecal}) are also close to the experimental ones (Q_{exp}), suggesting better fitting to the pseudo-second-order kinetic model. However, the relatively high values of regression coefficient (0.98) for the pseudo-first-order model could mean that physical adsorption was present, thus Hg^{2+} adsorption onto PTh/GO NC may have proceeded through a physicochemical process.

Table 2 | Non-linear kinetic models parameters for the adsorption of Hg^{2+} on PTh/GO NC

	Concentration (mg/L)		
Kinetic model/parameters	**50**	**100**	**200**
Q_{exp} (mg/g)	31.0	60.2	81.6
Pseudo-first-order			
Q_{ecal}, (mg/g)	33.46	67.49	89.13
k_1, (min^{-1})	0.085	0.035	0.030
R^2	0.988	0.984	0.997
Pseudo-second-order			
Q_{ecal} (mg/g)	31.7	60.4	79.3
k_2 (g mg^{-1} min^{-1})	3.5×10^{-3}	0.7×10^{-3}	0.5×10^{-3}
h (mg g^{-1} min^{-1})	3.52	2.55	3.14
R^2	0.997	0.990	0.989

Competitive adsorption

Industrial wastewater comprises a mixture of many ions that may influence the selectivity of the desired ions. Consequently, the effect of binary, ternary and multicomponent ions on the adsorption of Hg^{2+} ions onto PTh/GO NC was investigated. The experiments with mixtures of co-ions (Cu^{2+}, Mn^{2+}, Zn^{2+}) in Figure 7 show that the hydrated metal ions may significantly alter the adsorption efficiency of the PTh/GO NC over Hg^{2+}. There is a competition of

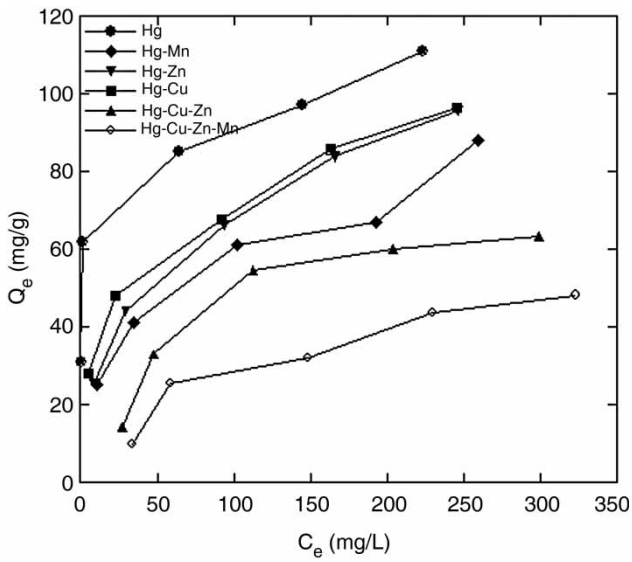

Figure 7 | Equilibrium curves for selectivity of Hg^{2+} ion in single, binary, ternary and multicomponent systems.

the free and hydrated Hg ions with the larger metal ions in the solution (dependence with the hydraulic radii of the ions). Co-ions affected Hg^{2+} removal in this order: Mn > Zn > Cu.

Desorption experiments

Desorption and regeneration of an adsorbent is an important undertaking from the applicability and the economic point of view because they relate to the overall treatment cost. Moreover, regeneration helps elucidate the adsorption mechanism. Figure 8(a) shows the efficacy of different eluents on the desorption of Hg^{2+} from the spent PTh/GO NC. The high elution efficiency ca. 90% obtained using 0.5 M HCl can be attributed to its ability to form special complexes with Hg^{2+} ions, such as $HgCl^{+}$, $HgCl_2$, $HgCl^{3-}$ and $HgCl^{4-}$ (Chen *et al.* 2015). Therefore further desorption tests were carried out using 0.5 M HCl with 1 M NaOH used to activate the regenerated PTh/GO NC. Results in Figure 8(b) shows that the Hg^{2+} removal efficiency increased after repeatedly treating the PTh/GO NC with both the acid and alkali. Further, the NC could be reused for three adsorption-desorption cycles without significant loss of adsorption capacity. The regeneration results suggested that the adsorption process may have involved ion-exchange or weak chemisorption such as chelation.

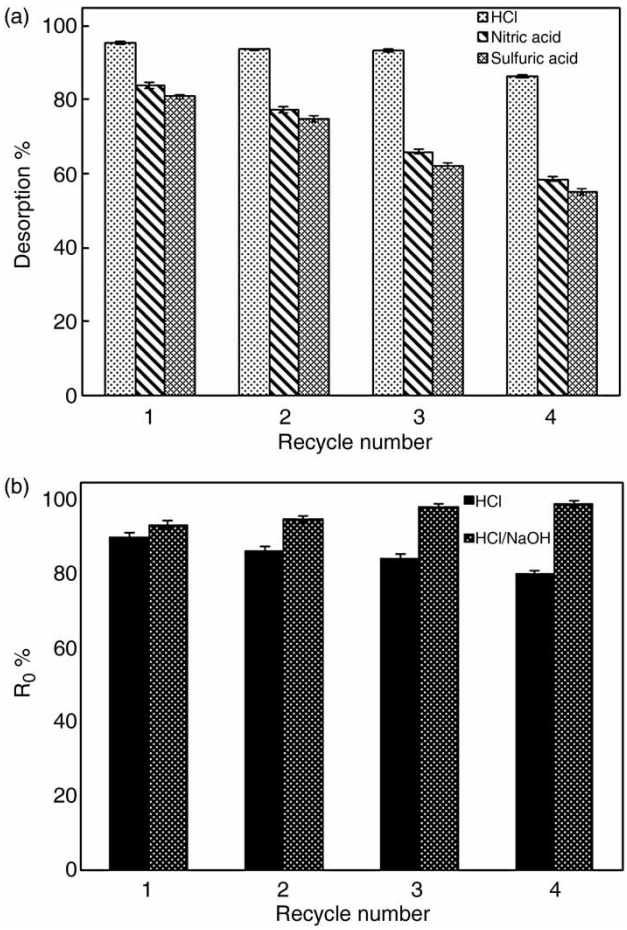

Figure 8 | Adsorption-desorption studies (a) desorption efficiency with different eluents and (b) removal efficiency after activation of HCl regenerated Hg^{2+}-loaded PTh/GO NC with NaOH (Co = 100 mg/L).

Adsorption mechanism

The adsorption of mercury ions onto PTh/GO NC can be considered to have proceeded via a complexation or chelation mechanism between S atoms of PTh/GO NC and the mercury ions, according to HSAB and ligand field theories (Pearson 1963). PTh is a chelating agent with S groups (soft base), and hence has very high affinity for mercury ions (soft acid). Thus, the 6 s unoccupied orbitals contained in mercury ions may be adsorbed by chelating with a lone pair of electrons available in the S atom of the PTh/GO NC through electron pair sharing, resulting in the formation of coordination compounds with a tetrahedral pattern. Also, it is possible that there could be some ion exchange and electrostatic attraction between Hg^{2+} and H^{+} and Hg^{2+} with OH^{-} considering the results on the effect of pH (protonation and deprotonation effects). The adsorption mechanism is further supported by the adsorption isotherms and kinetics models, which suggested that more than one mechanism was involved. Moreover, the FT-IR results showed a shift in C-S-C wavenumber and a change in the intensity and shape of the peaks after mercury adsorption, suggesting there was some interaction between the S atom and Hg^{2+} Similar results were reported by Tahmasebi *et al.* (2013) and Chen *et al.* (2015).

CONCLUSIONS

This study evaluated the performance of the prepared PTh/GO NC in the removal of Hg^{2+} ions from aqueous solutions. The uptake and equilibrium studies indicated that the adsorption of Hg^{2+} ions onto PTh/GO NC follows the Langmuir and Freundlich isotherms, while the kinetics fitted the pseudo-second-order model. The thermodynamic studies shows that the adsorption of Hg^{2+} onto PTh/NC is endothermic in nature and proceeded by physicochemical process. Further, the results from the adsorption-desorption studies indicated that HCl and NaOH could be used as eluent and activator, respectively, and the regenerated

adsorbent could be reused for three cycles without significant loss in its adsorption capacity. The main possible removal mechanisms involved were complexation, ion-exchange and neutralisation. These findings demonstrated that PTh/GO NC is a promising candidate material for mercury ion remediation.

ACKNOWLEDGEMENTS

Financial support was received from Rand Water, South Africa, through the Rand Water Chair in Water Utilisation (Tshwane University of Technology). We wish to gratefully acknowledge Jacob Kitinya for assisting in proofreading the manuscript.

REFERENCES

Bandaru, N. M., Reta, N., Dalal, H., Ellis, A. V., Shaptera, J. & Voelckerb, N. H. 2013 Enhanced adsorption of mercury ions on thiol derivatized single wall carbon nanotubes. *Journal of Hazardous Materials* **261**, 534–541.

Bhattacharya, I., Chakraborty, R. & Chowdhury, R. 2016 Biofilm reactor for Hg^{2+} removal: review with challenges and a study with freeze dried bacteria. *Journal of Environmental Engineering* **142** (9).

Bibby, A. & Mercier, L. 2002 Mercury (II) ion adsorption behavior in thiolfunctionalized mesoporous silica microspheres. *Chemistry of Materials* **14**, 1591–1597.

Bobade, R. S. 2011 Polythiophene composites: a review of selected applications. *Journal of Polymer Engineering* **31** (2–3), 209–215.

Carrott, P. J., Carrott, R. M. M. L. & Nabais, J. M. V. 1998 Influence of surface ionization on the adsorption of aqueous mercury chlorocomplexes by activated carbons. *Carbon* **30** (1–2), 11–17.

Chen, J., Feng, J. & Yan, W. 2015 Facile synthesis of a polythiophene/TiO_2 particle composite in aqueous medium and its adsorption performance for Pb(II). *RSC Advances* **5**, 86945–86953.

Chowdhury, S. & Saha, P. 2011 Adsorption kinetic modeling of safranin onto rice husk biomatrix using pseudo-first- and pseudo-second-order kinetic models: comparison of linear and non-linear methods. *Clean–Soil, Air, Water* **39** (3), 274–282.

Cui, L., Guo, X., Wei, Q., Wang, Y., Liang Gao, L., Yan, L., Yan, T. & Du, B. 2015 Removal of mercury and methylene blue from aqueous solution by xanthate functionalized magnetic graphene oxide: sorption kinetic and uptake mechanism. *Journal of Colloid and Interface Science* **439**, 112–120.

Ekinci, E., Budinova, T., Yardim, F., Petrov, N., Razvigorova, M. & Minkova, V. 2002 Removal of mercury ion from aqueous solution by activated carbons obtained from biomass and coals. *Fuel Processing Technology* **77–78**, 437–443.

Foo, K. Y. & Hameed, B. H. 2010 Insights into the modeling of adsorption isotherm systems. *Chemical Engineering Journal* **156**, 2–10.

Henneberry, Y. K., Kraus, T. E., Fleck, J. A., Krabbenhoft, D. P., Bachand, P. M. & Horwath, W. R. 2011 Removal of inorganic mercury and methylmercury from surface waters following coagulation of dissolved organic matter with metal-based salts. *Science of the Total Environment* **409**, 631–637.

Kinniburgh, D. & Jackson, M. 1978 Adsorption of mercury (II) by iron hydrous oxide gel. *Soil Science Society of America Journal* **42**, 45–47.

Knocke, W. R. & Hemphil, L. H. 1981 Mercury (II) sorption by waste rubber. *Water Research* **15**, 275–282.

Kumar, R., Singh, S. & Yadav, B. C. 2015 Conducting polymers: synthesis, properties and applications. *International Advanced Research Journal in Science, Engineering and Technology* **2** (11), 110–124.

Lee, S. J., Lee, J. M., Cho, H. Z., Koh, W. G., Cheong, I. W. & Kim, J. H. 2010 Poly(thiophene) nanoparticles prepared by Fe^{3+}-catalyzed oxidative polymerization: a size-dependent effect on photoluminescence property. *Macromolecules* **43**, 2484–2489.

Lottermoser, B. G. 2010 *Mine Wastes: Characterization, Treatment and Environmental Impacts*. Springer, Sydney, Australia.

Marcano, D. C., Kosynkin, D. V., Berlin, J. M., Sinitskii, A., Sun, Z., Slesarev, A., Alemany, L. B., Lu, W. & Tour, J. M. 2010 Improved synthesis of graphene oxide. *ACS Nano* **4** (8), 4806–4814.

Mehdinia, A., Khodaee, N. & Jabbari, A. 2015 Fabrication of graphene/Fe_3O_4@polythiophene nanocomposite and its application in the magnetic solid-phase extraction of polycyclic aromatic hydrocarbons from environmental water samples. *Analytica Chimica Acta* **868**, 1–9.

Moghaddam, H. K. & Pakizeh, M. 2015 Experimental study on mercury ions removal from aqueous solution by MnO_2/CNTs nanocomposite adsorbent. *Journal of Industrial and Engineering Chemistry* **21**, 221–229.

Nabais, J. V., Carrott, P. J. M., Carrott, M. M. L. R., Belchior, M., Boavida, D., Tatiana Diall, T. & Gulyurtlu, I. 2006 Mercury removal from aqueous solution and flue gas by adsorption on activated carbon fibres. *Applied Surface Science* **252**, 6046–6052.

Namasivayam, C. & Periasamy, K. 1993 Bicarbonate treated peanut hull carbon for mercury (II) removal from aqueous solution. *Water Research* **27** (11), 1663–1668.

Nuengmatcha, P., Mahachai, R. & Chanthai, S. 2014 Removal of Hg(II) from aqueous solution using graphene oxide as highly potential adsorbent. *Asian Journal of Chemistry* **26**, 85–88.

Pearson, G. R. 1963 Hard and soft acids and bases. *Journal of American Chemical Society* **85**, 3533–3539.

Qiu, H., Lv, L., Pan, B. C., Zhang, Q. J., Zhang, W. J. & Zhang, Q. X. 2009 Critical review in adsorption kinetic models. *Journal of Zhejiang University Science A* **10** (5), 716–724.

Raji, F. & Pakizeh, M. 2013 Study of Hg(II) species removal from aqueous solution using hybrid $ZnCl_2$-MCM-41 adsorbent. *Applied Surface Science* **282**, 415–424.

Saleh, T. A. 2015 Isotherm, kinetic, and thermodynamic studies on Hg(II) adsorption from aqueous solution by silica- multiwall

carbon nanotubes. *Environmental Science and Pollution Research* **22** (21), 16721–16731.

Setshedi, K. Z., Bhaumik, M., Onyango, M. S. & Maity, A. 2015 High-performance towards Cr(VI) removal using multi-active sites of polypyrrole–graphene oxide nanocomposites: batch and column studies. *Chemical Engineering Journal* **262**, 921–931.

Shafeeq, A., Muhammad, A., Sarfraz, W., Toqeer, A., Rashid, S. & Rafiq, M. K. 2012 Mercury removal techniques for industrial waste water. *World Academy of Science, Engineering and Technology* **6**, 12–26.

Sharma, A., Sharma, A. & Arya, R. K. 2015 Removal of mercury(II) from aqueous solution: a review of recent work. *Separation Science and Technology* **50**, 1310–1320.

Sheet, I., Kabbani, A. & Holail, H. 2014 Removal of heavy metals using nanostructured graphite oxide, silica nanoparticles and silica/graphite oxide composite. *Energy Procedia* **50**, 130–138.

Shen, J., Hu, Y., Shi, M., Lu, X., Qin, C., Li, C. & Ye, M. 2009 Fast and facile preparation of graphene oxide and reduced graphene oxide nanoplatelets. *Chemistry of Materials* **21**, 3514–3520.

Tahmasebi, E., Yamini, Y., Moradi, M. & Esrafili, A. 2013 Polythiophene-coated Fe_3O_4 superparamagnetic nanocomposite: synthesis and application as a new sorbent for solid-phase extraction. *Analytica Chimica Acta* **770**, 68–74.

USEPA 2007 *Treatment Technologies for Mercury in Soil, Waste, and Water*. US Environmental Protection Agency, Washington, DC.

USEPA 2014 Priority Pollutant List. US Environmental Protection Agency, Washington, DC. https://www.epa.gov/sites/production/files/2015-09/documents/priority-pollutant-list-epa.pdf (accessed 20 January 2017).

Uygun, A., Turkoglu, O., Sen, S., Ersoy, E., Yavuz, A. G. & Batir, G. G. 2009 The electrical conductivity properties of polythiophene/TiO_2 nanocomposites prepared in the presence of surfactants. *Current Applied Physics* **9**, 866–871.

Wajima, T. & Sugawara, K. 2011 Adsorption behaviors of mercury from aqueous solution using sulfur-impregnated adsorbent developed from coal. *Fuel Processing Technology* **92**, 1322–1327.

Wayne, E. J. J., Jones, W. E., Chiguma, J., Johnson, E., Pachamuthu, A. & Santos, D. 2010 Electrically and thermally conducting nanocomposites for electronic applications. *Materials* **3**, 1478–1496.

WHO 1990 *Environmental Health Criteria 101, Methylmercury*. World Health Organization, Geneva, pp. 68–102.

Yan, H., Li, H., Tao, X., Li, K., Yang, H., Li, A., Xiao, A. & Cheng, R. 2014 Rapid removal and separation of iron(II) and manganese(II) from micropolluted water using magnetic graphene oxide. *ACS Applied Materials and Interfaces* **6**, 9871–9880.

Yardim, M. F., Budinova, T., Ekinci, E., Petrov, N., Razvigorova, M. & Minkova, V. 2003 Removal of mercury (II) from aqueous solution by activated carbon obtained from furfural. *Chemosphere* **52**, 835–841.

Yu, J. G., Yue, B. Y., Wu, X. W., Liu, Q., Jiao, F. P., Jiang, X. Y. & Chen, X. Q. 2016 Removal of mercury by adsorption: a review. *Environmental Science and Pollution Research* **23** (6), 5056–5076.

First received 25 October 2016; accepted in revised form 6 March 2017. Available online 18 March 2017